Appl. Sci. **2015**, *5*, 910-925; doi:10.3390/app5040910

OPEN ACCESS

applied sciences

ISSN 2076-3417

www.mdpi.com/journal/applsci

Article

Double Properties of Novel Acylhydrazone Nanomaterials Based on a Conjugated System: Anion Binding Ability and Antibacterial Activity

Xuefang Shang [1,*], Wanli Li [2], Yaqian Feng [3], Xin Li [3] and Xiufang Xu [4]

[1] Department of Chemistry, Xinxiang Medical University, Xinxiang 453003, Henan, China

[2] Department of Immunity, Xinxiang Medical University, Xinxiang 453003, Henan, China; E-Mail: yxylwl@126.com

[3] School of Pharmacy, Xinxiang Medical University, Xinxiang 453003, Henan, China; E-Mails: 15836077038@163.com (Y.F.); 15836165125@163.com (X.L.)

[4] Department of Chemistry, Nankai University, Tianjin 300071, China; E-Mail: xxfang@nankai.edu.cn

* Author to whom correspondence should be addressed; E-Mail: xuefangshang@126.com; Tel.: +86-373-302-9128, Fax: +86-373-302-9959.

Academic Editor: Philippe Lambin

Received: 15 August 2015 / Accepted: 12 October 2015 / Published: 21 October 2015

Abstract: A series of new compounds (**1**–**12**) containing 1,5-diaza-fluorenone, 1,10-phenanthroline-5,6-dione, ferrocene-1,1′-dione, anthracene-9-carbaldehyde have been synthesized and optimized. The nanomaterials were also developed successfully. The binding properties were evaluated for biologically important anions (F^-, Cl^-, Br^-, I^-, AcO^-, and $H_2PO_4^-$) by theoretical investigation, UV-vis, and fluorescence experiments, and compound **6** displayed the strongest binding ability for AcO^- ion among the synthesized compounds. Theoretical investigation analysis revealed that the intramolecular hydrogen bond existed in the structure of compound **6** and the roles of molecular frontier orbitals in molecular interplay. In addition, compound **6** showed wide antibacterial activity for colon bacillus, typhoid bacillus, and *Pseudomonas aeruginosa*, and inferior activity for hay bacillus and *Staphylococcus aureus*. This series of acylhydrazone nanomaterials showed double properties, anion binding ability, and antibacterial activity.

Keywords: binding ability; antibacterial activity; acylhydrazone derivative; nanomaterials; synthesis

1. Introduction

Selective recognition and sensing of biologically important anions has attracted considerable attention in the field of supramolecular chemistry because of its important roles in medical, biological, chemical, and environmental systems [1–10]. For example, carboxylate ions are vital components of many human metabolic processes [11]. Phosphorylated species are of considerable interest due to their existence in a variety of biological processes such as energy transduction, signal processing, genetic information storage, and membrane transport [12–14]. Thus, the importance of the selective detection of carboxylate and phosphorylated biomolecules probably surpasses that of other biologically functional anions. So far, the focus has mainly been on the design of a receptor that has the ability to recognize and bind the biologically important anions. The binding units in receptors are important and often composed of amide [15], urea [16], hydroxyl [17,18], and pyrrole [19] owing to their capacity to perform as hydrogen donors. However, the literature has reported few cases of acylhydrazone (NHCO) serving as an anion binding site.

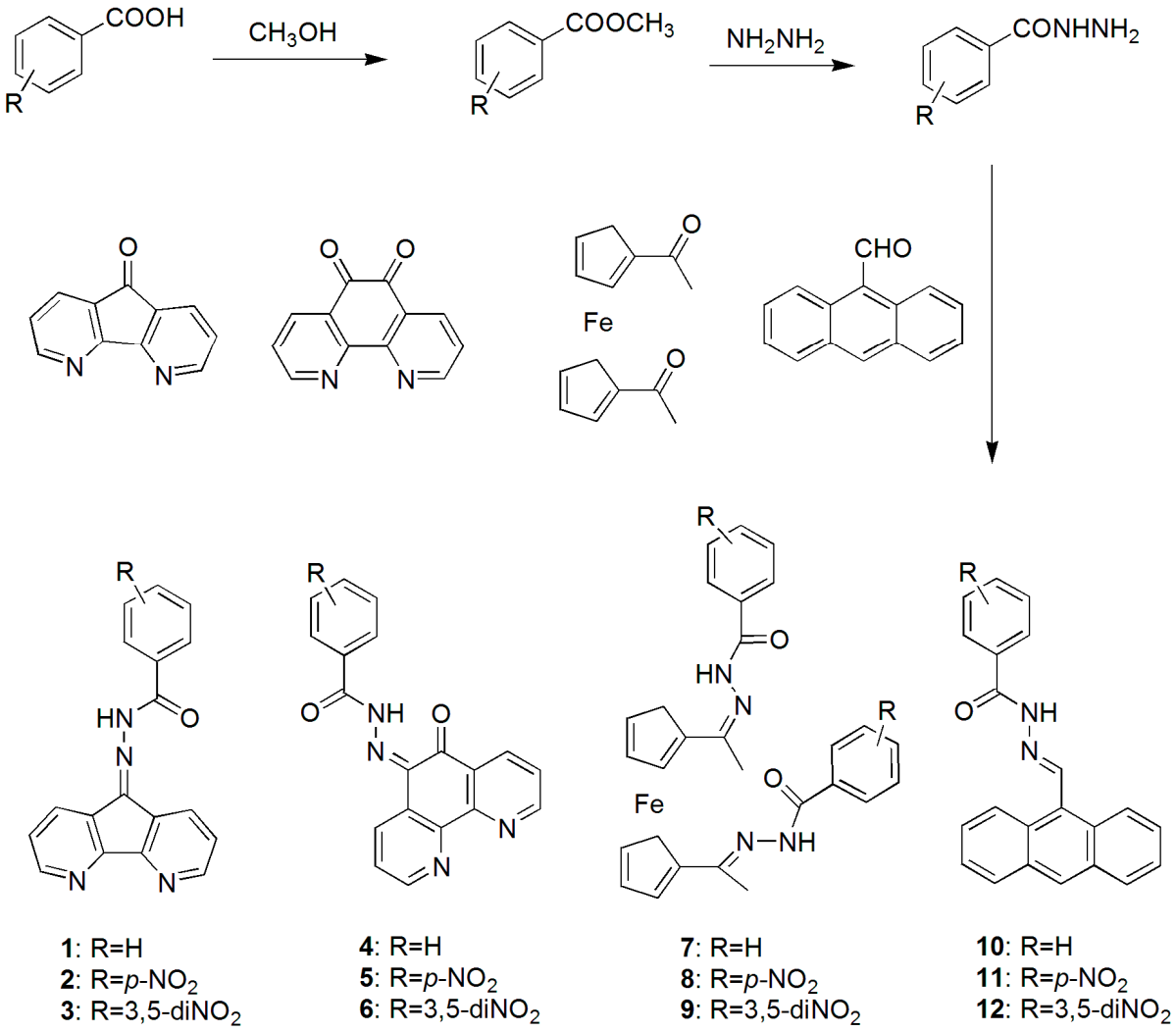

Scheme 1. Synthesis route for compounds.

The compounds containing a hydrazine structural unit have a molecular structure that is widely used as a precursor or intermediate of many organic molecules. A hydrazide skeleton is an important synthesis

unit and its derivatives also have great potential application because of their wide range of biological and physiological activity, including antiviral, antitumor, resistance to malaria, insecticide, and germicide [20–22]. Meanwhile, the strong coordination capacity makes it widely used in the analysis of subject areas, and for cyclic or non-cyclic hydrazide derivatives. Therefore, the synthesis and biological properties of hydrazine derivatives attracted the attention of many scholars. The research about the relationship between structure and biological activity could provide useful information in order to explore the sterilization of high effect and low toxicity drugs. However, almost no studies about anion binding ability based on acylhydrazone derivatives are currently being reported.

Bearing the above considerations in mind, in this paper we report the synthesis of benzoylhydrazine derivatives and their properties containing antibacterial activity and anion binding ability (Scheme 1). The obtained experimental results showed that compound **6** (phenanthroline hydrazide derivative) could effectively recognize and sense AcO^- in DMSO. To our delight, compound **6** also showed wide antibacterial activity.

2. Results and Discussion

2.1. SEM Images of Compounds

New attempt to synthesize nanomaterials of the synthesized compounds. Fortunately, nanomaterials of eight compounds (**1**, **2**, **4**, **5**, **7**, **8** and **11**) were prepared successfully. The SEM images were obtained by Quanta TM450 FEI after coating it with Au (Figure 1). As shown in Figure 1, three compounds (**1**, **4** and **5**) could be assembled into long, thin flakes on the entire compound. The thickness of flakiness was nano-size according to the scale. Compound **2** formed rectangular blocks. Two compounds (**7** and **11**) both formed squares. Compound **10** formed a himantioid shape. For compound **8** containing a *p*-NO_2 group in the ferrocene framework, the size of the particle was uniform and very small. Therefore, we also determined the nanomaterial using a field emission scanning electron microscope, which showed as **8′**. Clearly, compound **8** formed thin flakes. In general, all materials formed flakes or blocks except compound **10**, which contained anthracene and a nitro group. The width sizes of materials were a bit large and came to micro grade, while the thickness sizes were nano grade except compound **11**.

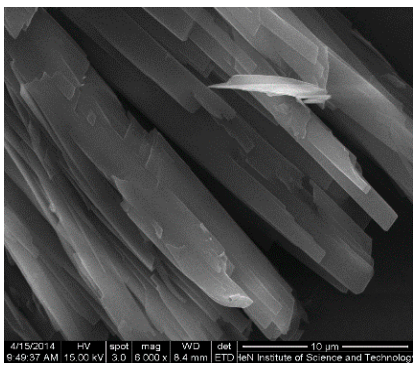

(**1**)

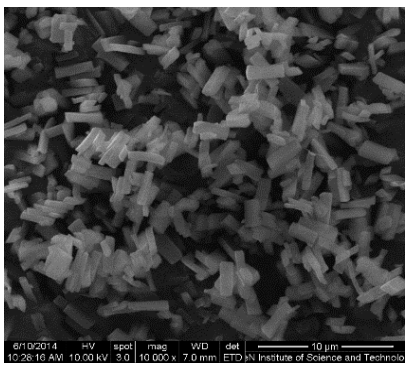

(**2**)

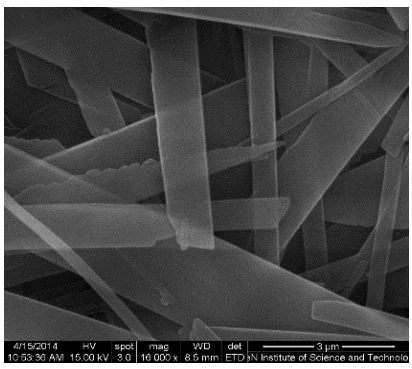

(**4**)

Figure 1. *Cont.*

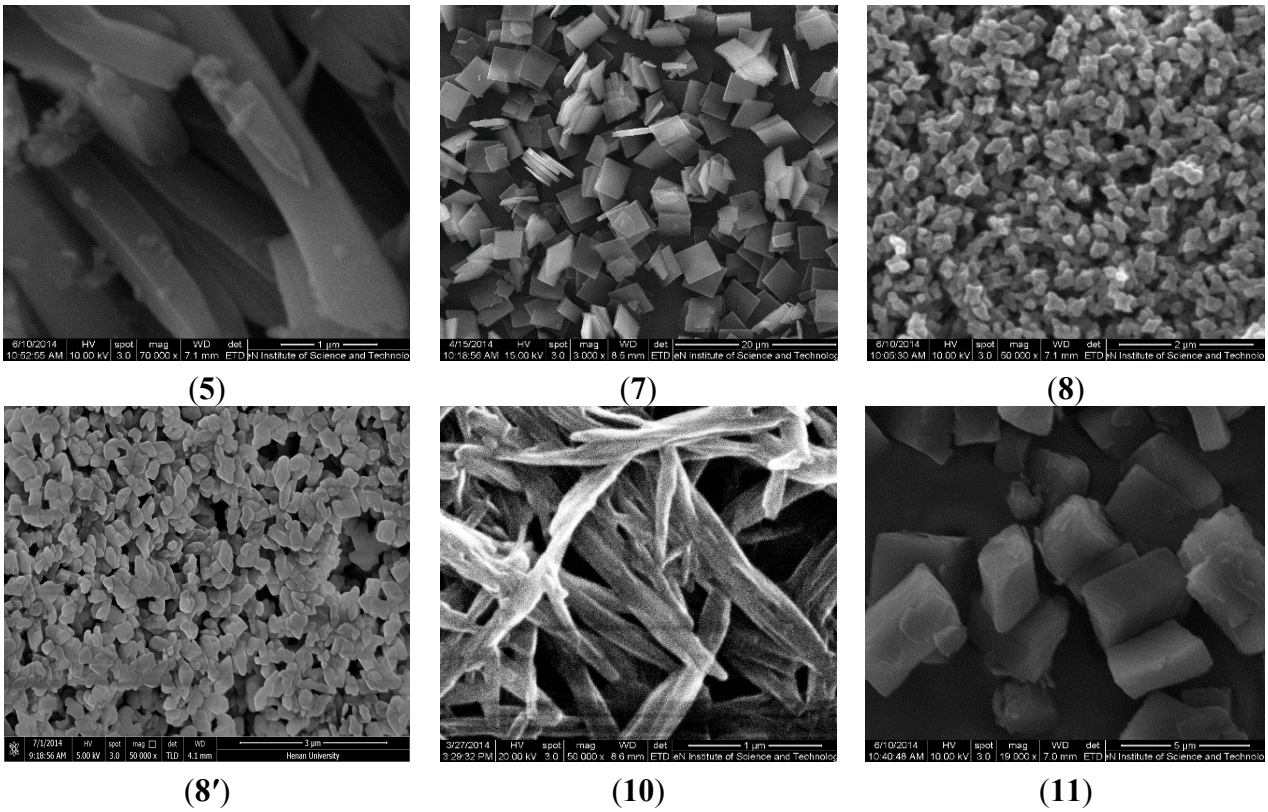

Figure 1. SEM images for compounds (**1**, **2**, **4**, **5**, **7**, **8**, **8′**, **10** and **11**).

2.2. UV-Vis Titration

The anion binding abilities of 12 compounds (**1**–**12**) were investigated in detail through UV-vis spectroscopy in DMSO. Results indicated that only six compounds (**1**, **2**, **3**, **6**, **9** and **11**) showed binding ability for anions. The UV-vis spectral changes of six compounds (4.0×10^{-5} mol·L^{-1}) upon the titration with acetate anion are shown in Figure 2. As seen in Figure 2, the spectra of free **1** exhibited a strong absorption band centered at 350 nm and a weak absorption band centered at 437 nm. With the stepwise addition of acetate anion to the solution of compound **1**, the strong absorbance band at 350 nm decreased in intensity and the sharp peak thoroughly disappeared. At the same time, the weak wide absorbance band centered at 437 nm increased gradually and developed a sharp peak. In general, the red-shift phenomenon in absorption spectra was induced by the addition of acetate anion to compound **1**. The reason may be that the conjugative effect between the host and guest was strengthened after the hydrogen bond formed between compound **1** and acetate anion [23,24]. One clear isosbestic point at 375 nm appeared, which indicated that a stable complex having a certain stoichiometric ratio had formed between **1** and acetate anion [25]. Particularly, the presence of F^- and $H_2PO_4^-$ induced similar changes in the UV-vis spectra of **1** compared with AcO^- (the spectra listed in the supplementary information Figure S1). However, the addition of excess equivalents of Cl^-, Br^-, and I^- resulted in slight changes in the absorption spectrum. The above results indicated that compound **1** showed a different binding ability with F^-, AcO^-, and $H_2PO_4^-$, and almost no or a very weak binding ability with Cl^-, Br^-, and I^-. For compounds **2** and **3**, similar spectral changes were induced by the addition of an acetate anion due to the similar structures (1,5-diaza-fluorenone derivatives). However, compounds **6** (1,10-phenanthranol-5,6-dione), **9** (ferrocene-1,1′-dione), and **11** (anthracene-9-carbaldehyde) showed a different spectral response due

to the different framework, while a similar red-shift phenomenon appeared in the host-guest interaction process.

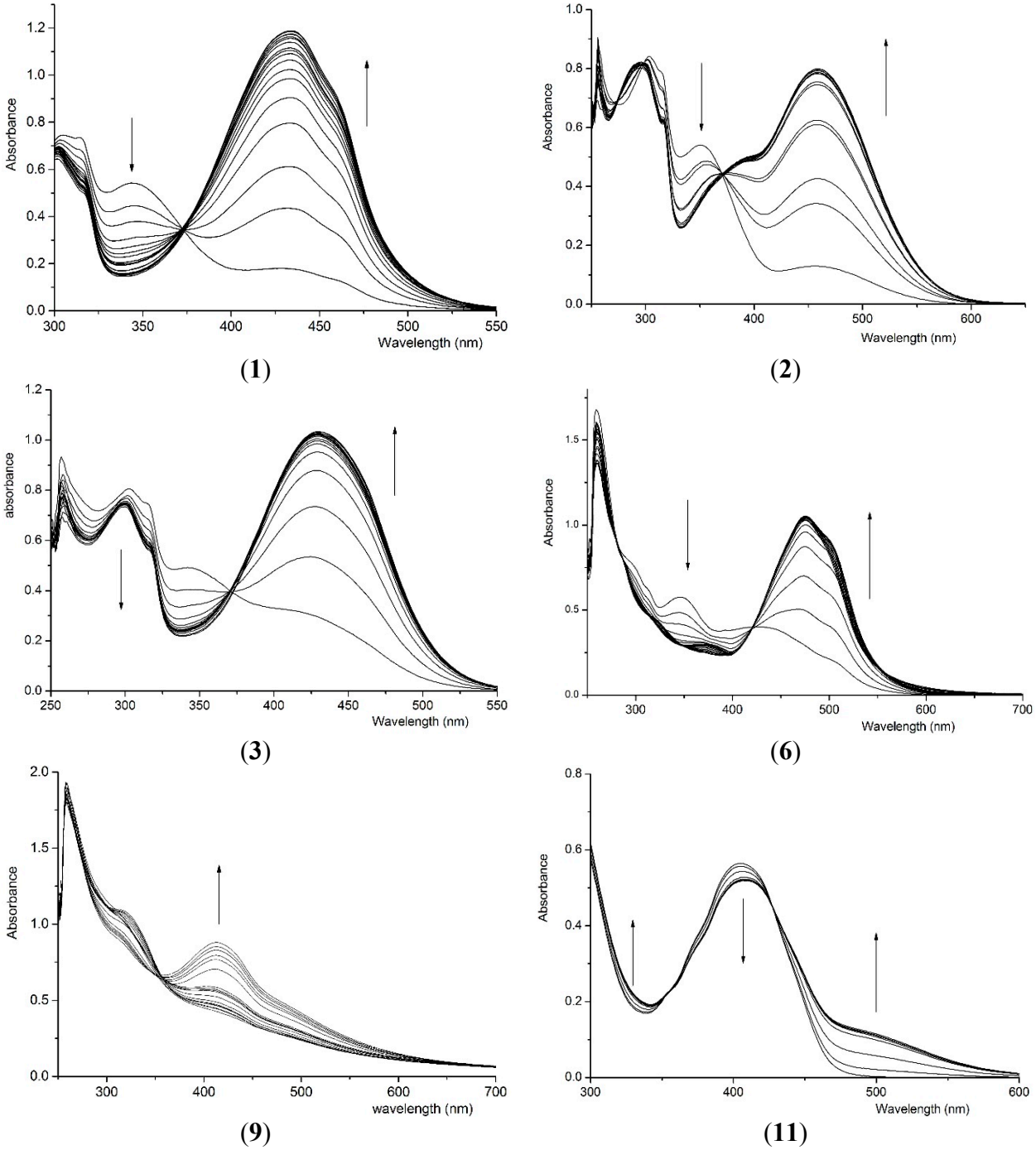

Figure 2. UV-vis spectral changes of various compounds upon the addition of an acetate anion compounds (**1**, **2**, **3**, **6**, **9** and **11**). (compound) = 4.0×10^{-5} mol·L^{-1}; (acetate anion) = -1.6×10^{-3} mol·L^{-1}. Arrows indicate the direction of increasing anion concentration.

2.3. Fluorescence Response

The photophysical responses of six compounds (**1**, **2**, **3**, **6**, **9** and **11**) toward the addition of anions tested were also investigated. Just as Figure 3 showed, the fluorescence spectra of compound **1** exhibited a very weak response. Upon the addition of acetate anion (0–50 equiv.) to the solution of compound **1**, the fluorescence centered at 430 nm was enhanced. To account for such fluorescence enhancement, the PET mechanism was exploited [26–28]. In the case of compound **1**, the excited state of the fluorophore was not, or only to a minor extent, enhanced by electron transfer (ET) from the receptor to the fluorophore and the receptor–anion interaction. The addition of F^- and $H_2PO_4^-$ induced similar fluorescence enhancement (the spectra are listed in the supplementary information Figure S2). Nevertheless, the fluorescence emission of compound **1** was insensitive to the additions of excess equivalents of Cl^-, Br^-, and I^- ions, which indicated the weak interaction.

In view of the fluorescence titration spectra of other compounds (**2**, **3**, **6**, **9**, and **11**), the fluorescence intensity was enhanced for all of them due to the increase in acetate anion concentration (Figure 3), which indicated that the above compounds interacted with the acetate anion. The addition of $H_2PO_4^-$ and F^- induced similar fluorescence enhancement for compounds **2**, **3**, and **6** (the spectra are listed in the supplementary information Figure S2). Compound **9** showed different binding ability for AcO^- and $H_2PO_4^-$, while, compound **11** only showed binding ability for AcO^-. The addition of Cl^-, Br^-, and I^- aroused very weak fluorescence enhancement and the interaction of host and guest could be ignored.

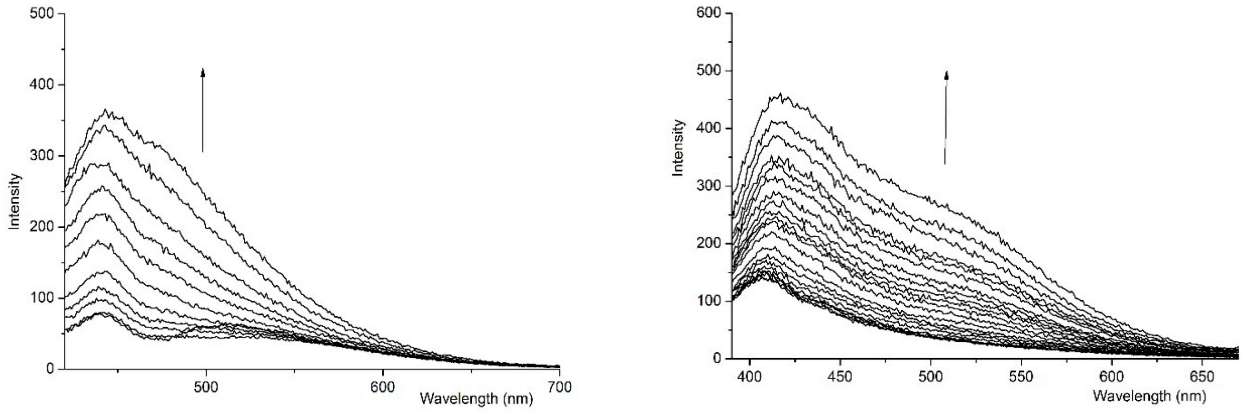

(**1**) (**2**)

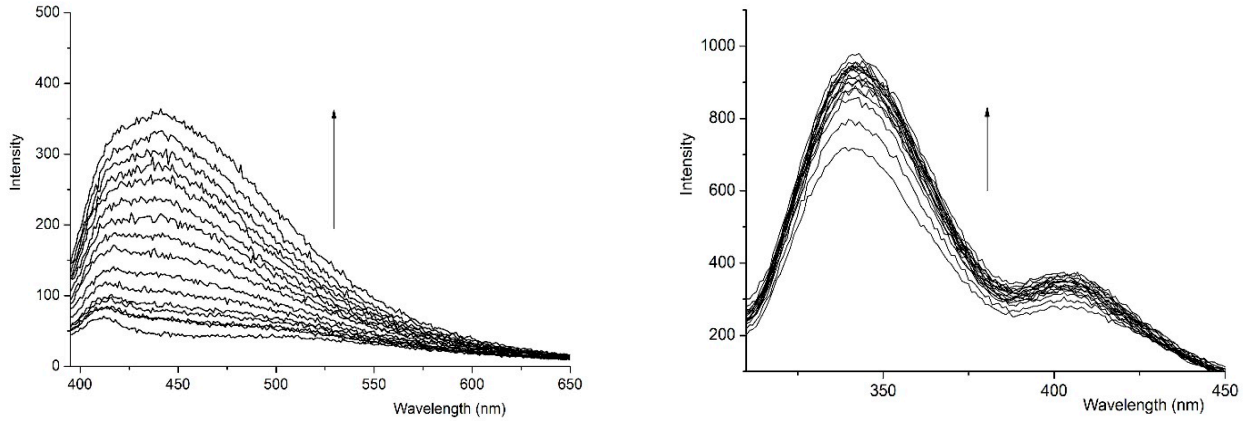

(**3**) (**6**)

Figure 3. *Cont.*

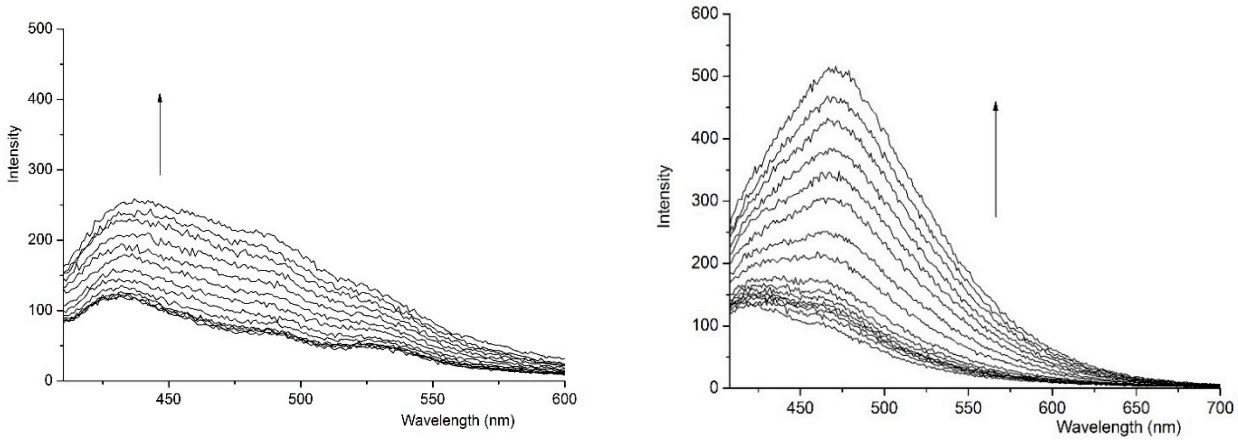

Figure 3. Fluorescence response of compounds (**1**, **2**, **3**, **6**, **9** and **11**) (4.0×10^{-5} mol·L^{-1}) upon the addition of an acetate anion (-2.0×10^{-3} mol·L^{-1}); arrows indicate the increasing direction of the acetate anion concentration.

2.4. Binding Constant

The above analyses indicated that the spectral change could be ascribed to the formation of 1:1 host-guest complexation. The obtained binding constants were calculated using the method of non-linear least squares according to the UV-vis data and listed in Table 1 [29,30]. According to Table 1, the binding constants of compounds **4**, **5**, **7**, **8**, **10** and **12** with various anions cannot be calculated due to the very weak spectral changes and the binding ability can be ignored. The binding trend of six compounds (**1**, **2**, **3**, **6**, **9** and **11**) to anions was as follows: $AcO^- > H_2PO_4^- > F^- >> Cl^- \sim Br^- \sim I^-$. It was apparent that the sensitivity for multiple hydrogen-bond interactions could be rationalized on the basis of the interaction between the host and the anionic guest. As expected from their basicity, AcO^-, $H_2PO_4^-$ and F^- bound more strongly than the other anions tested. In general, the AcO^- ion showed the strongest binding ability with the above compounds. For the acetate ion, the binding ability followed the order of: **6** > **3** > **2** > **1** > **11** > **9**. That is, 1,10-phenanthroline-5,6-dione derivatives containing dinitro groups showed the strongest binding ability among the synthesized compounds. The reason might be that the electron-withdrawing group could strengthen the acidity of the compound and the binding ability increased correspondingly. As for anthracene-9-carbaldehyde derivatives (**10**, **11** and **12**), compound **11** containing one nitro group showed high sensitivity, while compound **12** involving dinitro groups showed almost no binding ability for the acetate anion. The reason may be related to steric hindrance.

Table 1. Binding constants of compounds with various anions.

Anion	AcO^-	$H_2PO_4^-$	F^-
K_s (**1**)	$(5.69 \pm 0.56) \times 10^5$	$(2.14 \pm 0.17) \times 10^4$	$(1.02 \pm 0.11) \times 10^4$
K_s (**2**)	$(4.35 \pm 0.41) \times 10^6$	$(1.39 \pm 0.89) \times 10^6$	$(1.49 \pm 0.38) \times 10^6$
K_s (**3**)	$(8.40 \pm 0.78) \times 10^6$	$(2.73 \pm 0.21) \times 10^4$	$(7.32 \pm 0.03) \times 10^3$
K_s (**4**)	ND	ND	ND
K_s (**5**)	ND	ND	ND

Table 1. *Cont.*

Anion	AcO^-	$H_2PO_4^-$	F^-
K_s (**6**)	$(1.83 \pm 0.60) \times 10^7$	$(1.81 \pm 0.32) \times 10^4$	$(1.43 \pm 0.02) \times 10^3$
K_s (**7**)	ND	ND	ND
K_s (**8**)	ND	ND	ND
K_s (**9**)	$(1.26 \pm 0.09) \times 10^3$	$(4.45 \pm 0.45) \times 10^2$	ND
K_s (**10**)	ND	ND	ND
K_s (**11**)	$(4.12 \pm 0.10) \times 10^4$	ND	ND
K_s (**12**)	ND	ND	ND

ND: The spectrum change little and the binding constant cannot be calculated.

2.5. Antibacterial Activity

The antibacterial activity of the synthesized compounds (**4**, **5**, **6**, **10**, **11** and **12**) was tested by the filter paper method (Figure 4). The reference solution did not show antibacterial activity for the bacteria tested. As shown in Figure 4, six compounds showed wide antibacterial activity, especially for colon bacillus, typhoid bacillus, and *Pseudomonas aeruginosa*. However, they all showed very weak sensitivity for hay bacillus and *Staphylococcus aureus*, which could be ignored. The antibacterial activity of compound **6** and **12** was especially strong in the synthesized compounds. The above results could provide reference data for further study of the antibacterial activity of acylhydrazone based on 1,10-phenanthroline-5,6-dione and 9-anthracene derivatives.

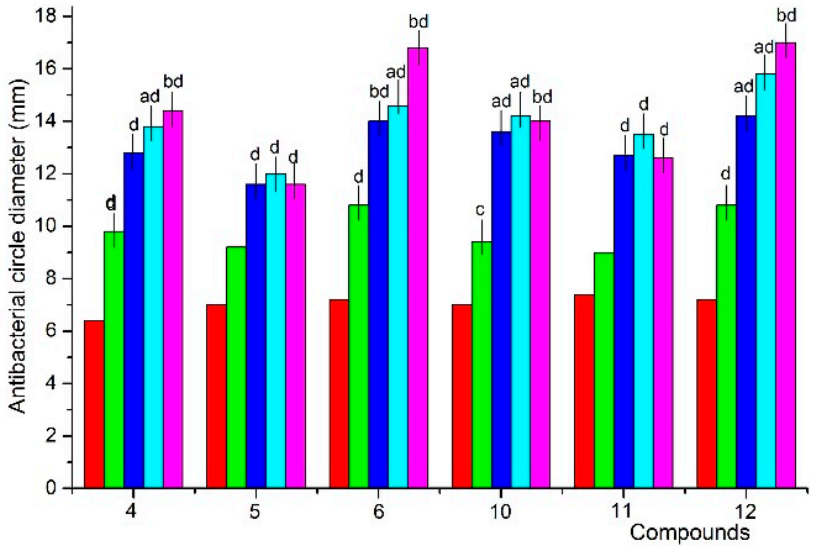

Figure 4. Antibacterial circle for compounds **4**, **5**, **6**, **10**, **11**, and **12**; a: compared with **4**, $p < 0.05$; b: compared with **4**, $p < 0.01$; c: compared with hay bacillus, $p < 0.05$; d: compared with hay bacillus, $p < 0.01$; ad: compared with **4**, $p < 0.05$, and compared with Bacillus $p < 0.01$; bd: compared with **4**, $p < 0.01$, and compared with Bacillus $p < 0.01$. Red column: hay bacillus; green column: *Staphylococcus aureus*; blue column: colon bacillus; light blue: typhoid bacillus; pink column: *Pseudomonas aeruginosa*.

2.6. Theoretical Investigation

The geometries of five compounds (**1**, **2**, **3**, **6** and **11**) were optimized (Figure 5) using the HF (Hartree-Fock) method with the basis sets 3–21G. The calculation was performed with the Gaussian 03 program [31]. From Figure 5, the intramolecular hydrogen bond only existed in compound **6**, in which the distance between the hydrogen atom of the interacted site (-NH) and the oxygen atom of ketone group was 1.667 Å. The intramolecular hydrogen bond did not exist in other compounds (**1**, **2**, **3** and **11**). According to the literature [32,33], the existence of an intramolecular hydrogen bond could improve the anion binding ability and so the anion binding ability of compound **6** was the strongest of the synthesized compounds. The above results indicate that multiple hydrogen bonds are important to anion binding ability.

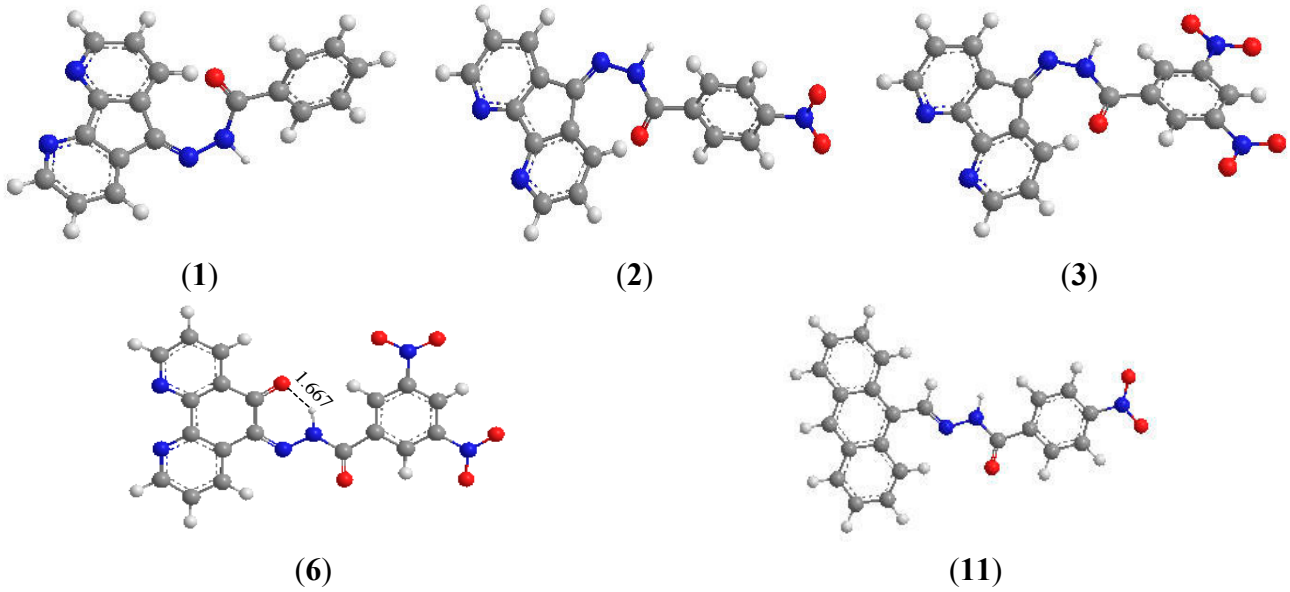

Figure 5. The optimized structures of synthesized compounds (**1**, **2**, **3**, **6** and **11**).

In addition, selected frontier orbitals for the synthesized compounds (**1**, **2**, **3**, **6** and **11**) were shown in Figure 6. We introduced molecular frontier orbital in order to explain the red-shift phenomenon of UV-vis absorption spectra in the host–guest interaction process by electron transition of the frontier orbital. For compound **1**, the highest occupied molecular orbital (HOMO) density was mainly localized on the 5-diaza-fluorenone moiety, while the lowest unoccupied molecular orbital (LUMO) density was localized on the whole molecular, which demonstrated that it was the electron transition of HOMO to arouse the red-shift phenomenon in the UV-vis spectra of host–guest. A similar result was also observed in compound **6**. For compounds **2**, **3** and **11**, the HOMO density was mainly localized on the 5-diaza-fluorenone moiety and 9-anthracene moieties, while the LUMO density was localized on the benzene cycle moiety, which demonstrated it was the electron transition of HOMO to arouse the red shift phenomenon. In addition, the frameworks of compounds **1**–**3** were identical based on 5-diaza-fluorenone derivatives. However, the electron cloudy densities were different due to the different substituent.

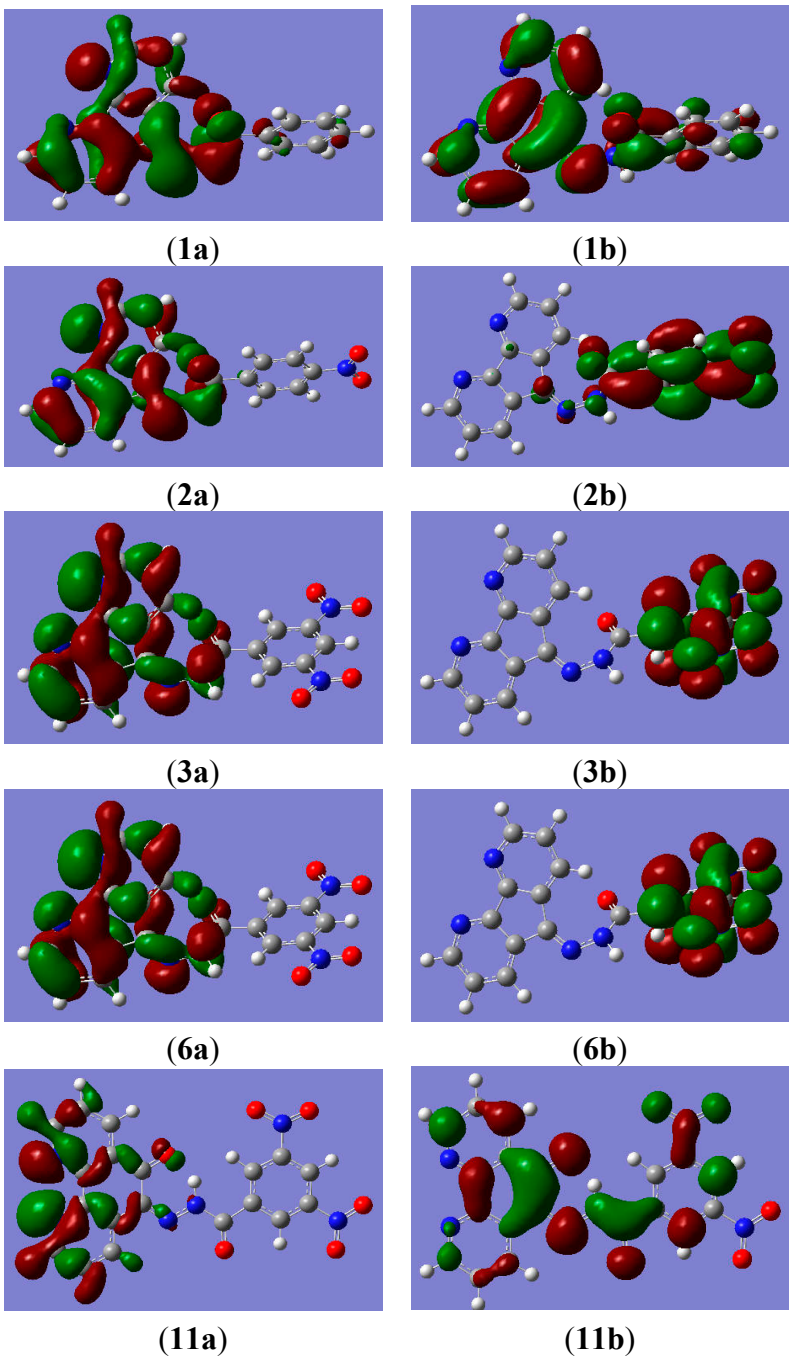

Figure 6. Selected HOMO (**a**); and LUMO (**b**) distributions of **1**, **2**, **3**, **6** and **11**.

3. Experimental Section

Most of the starting materials were obtained commercially and all reagents and solvents used were of analytical grade. Hydrazine sulfate and all anions, in the form of tetrabutylammonium salts (such as (n-C_4H_9)$_4$NF, (n-C_4H_9)$_4$NCl, (n-C_4H_9)$_4$NBr, (n-C_4H_9)$_4$NI, (n-C_4H_9)$_4$NAcO, (n-C_4H_9)$_4$$NH_2PO_4$), were purchased from Aladdin Chemistry Co. Ltd (Shanghai, China), stored in a desiccator under a vacuum containing self-indicating silica, and used without any further purification. Tetra-n-butylammonium salts were dried for 24 h in a vacuum with P_2O_5 at 333 K before using. Dimethyl sulfoxide (DMSO) was distilled *in vacuo* after being dried with CaH_2. C, H, N elemental analysis was made on Vanio-EL (Heraeus, Hanau, Germany). ^{1}H NMR spectra was recorded on a Varian Plus-400 MHz Spectrometer

(Bruker, Germany). ESI-MS was performed with a LC-MS apparatus (Agilent, Santa Clara, CA, USA). UV-vis spectroscopy titration was made on a Shimadzu UV2550 spectrophotometer (Japan) at 298 K. Fluorometric titration was performed on a Cary Eclipse Fluorescence Spectrophotometer (Agilent, Santa Clara, CA, USA) at 298 K. The binding constant (K_s) was obtained by non-linear least square calculation method for data fitting. The SEM images were obtained by Quanta TM450 FEI (Agilent, Santa Clara, CA, USA) coating it with Au. The kinds of bacteria were hay bacillus, *Staphylococcus aureus*, colon bacillus, typhoid bacillus, and *Pseudomonas aeruginosa*. Antibacterial activity was determined by filter paper method. The qualitative filter paper was made into small round pieces (Φ = 6 mm), used after high pressure sterilization. The filter paper was placed in saline water for 2 h as a reference solution. Under the sterile conditions, the appropriate culture medium (20–25 mL) was dished into a sterilized Petri and made into a solid plate after solidifying. The prepared bacterial suspension (200 μL) was poured into the appropriate solid medium using rods with a liquid coating. The filter paper was pasted on the bacterial plate. The essential oils (5 μL) were added onto each piece of filter paper. Colon bacillus, *Staphylococcus aureus*, hay bacillus, typhoid bacillus, and *Pseudomonas aeruginosa* were placed in a culture incubator (37 °C) for 24 h. Then the data of antibacterial circle diameter was the difference between the measured value and reference value. Therefore, the experimental data of antibacterial circle diameter showed the antibacterial activity of various bacteria.

Twelve compounds (**1**–**12**) were synthesized according to the route shown in Scheme 1.

Substituted methyl benzoate was synthesized according to the literature [34]. Substituted benzoic acid (10 mmol), dissolved in methanol (20 mL) and concentrated sulfuric acid (0.5 mL), was added into the above solution. The above mixture was refluxed for 3 h and then the precipitated solid was obtained.

Substituted benzohydrazide was synthesized according to the literature [35,36]. Substituted methyl benzoate (10 mmol), dissolved in methanol and hydrazine hydrate (80%, 2 mL), was added to the solution. Then the mixture was heated under refluxing for 6 h and the precipitate was separated by filtration. The solid was recrystallized using 95% ethanol, washed with diethyl ether, and dried under a vacuum.

Benzohydrazide: m.p. 111–114 °C.

p-Nitrobenzohydrazide: m.p. 214–217 °C. ^{1}H NMR (DMSO-d_6): δ 10.11 (t, 1H), 8.29 (d, 2H), 8.04 (d, 2H), 4.76 (d, 2H)

3,5-Dinitrobenzohydrazide: m.p. 229–231 °C. ^{1}H NMR (DMSO-d_6): δ 9.90 (t, 1H), 7.72 (s, 1H), 7.47 (s, 1H), 7.37 (s, 1H), 4.50 (d, 2H)

Twelve compounds (**1**–**12**) were synthesized according to the following method. Substituted benzohydrazide (1 mmol) was dissolved in dry ethanol (30 mL). 1,5-diaza-fluorenone, 1,10-phenanthroline-5,6-dione, ferrocene-1,1′-dione, anthracene-9-carbaldehyde (1 mmol), dissolved in dry ethanol (20 mL), was added into the above solution. Then the mixture was heated under refluxing for 4 h and the precipitate was separated by filtration. The solid was recrystallized using ethanol, washed with diethyl ether, and dried under a vacuum.

Compound **1**: Yield: 87%. m.p. > 320 °C. ^{1}H NMR (400 MHz, DMSO-d_6, 298 K) δ 12.05 (s, 1H), 8.76–8.72 (m, 2H), 8.55 (d, 1H), 8.23 (d, 1H), 8.03 (d, 2H) 7.65–7.48 (m, 5H). Elemental analysis: Calc. for $C_{18}H_{12}N_4O$: C, 71.99; H, 4.03; N, 18.66; Found: C, 71.84; H, 4.39; N, 18.91. ESI-MS (*m*/*z*): 299.3 $(M - H)^-$.

Compound **2**: Yield: 83%. m.p. > 320 °C. ^{1}H NMR (400 MHz, DMSO-d_6, 298 K) δ 12.24 (s, 1H), 8.76–8.72 (m, 2H), 8.60 (d, 1H), 8.39 (d, 2H), 8.25–8.19 (m, 3H), 7.56–7.47 (m, 2H). Elemental analysis: Calc. for $C_{18}H_{11}N_5O_3$: C, 62.61; H, 3.21; N, 20.28; Found: C, 63.02; H, 3.58; N, 20.47. ESI-MS (*m*/*z*): 344.2 $(M - H)^-$.

Compound **3**: Yield: 80%. m.p. > 320 °C. ^{1}H NMR (400 MHz, DMSO-d_6, 298 K) δ 12.08 (s, 1H), 8.76–8.73 (t, 2H), 8.51 (d, 1H) 8.23 (d, 1H), 7.92 (s, 1H), 7.60–7.47 (m, 4H), 6.10 (s, 2H). Elemental analysis: Calc. for $C_{18}H_{10}N_6O_5$: C, 55.39; H, 2.58; N, 21.53; Found: C, 55.44; H, 2.96; N, 21.62. ESI-MS (*m*/*z*): 389.0 $(M - H)^-$.

Compound **4**: Yield: 91%. m.p. 236–239 °C. ^{1}H NMR (400 MHz, DMSO-d_6, 298 K) δ 11.32 (s, 1H), 10.19 (s, 1H), 9.42 (d, 2H), 8.97 (d, 1H), 8.91 (t, 1H), 8.55 (t, 1H), 8.38 (d, 1H), 7.69 (m, 5H). Elemental analysis: Calc. for $C_{19}H_{12}N_4O_2$: C, 69.51; H, 3.68; N, 17.06; Found: C, 69.25; H, 3.87; N, 16.95. ESI-MS (*m*/*z*): 327.2 $(M - H)^-$.

Compound **5**: Yield: 88%. m.p. 247–250 °C. ^{1}H NMR (400 MHz, DMSO-d_6, 298 K) δ 11.58 (s, 1H), 9.43 (s, 1H), 9.10 (d, 2H), 8.90 (t, 2H), 8.56 (d, 2H), 7.71 (m, 4H). Elemental analysis: Calc. for $C_{19}H_{11}N_5O_4$: C, 35.20; H, 1.72; N, 23.94; Found: C, 35.48; H, 1.93; N, 23.57. ESI-MS (*m*/*z*): 376.2 $(M - H)^-$.

Compound **6**: Yield: 84%. m.p. 306–308 °C. ^{1}H NMR (400 MHz, DMSO-d_6, 298 K) δ 15.15 (s, 1H), 9.09 (d, 2H), 8.88 (d, 2H), 8.61 (t, 2H), 7.80 (s, 1H), 7.73 (s, 1H), 7.64 (s, 1H). Elemental analysis: Calc. for $C_{19}H_{10}N_6O_6$: C, 54.55; H, 2.41; N, 20.09; Found: C, 54.60; H, 2.76; N, 20.41. ESI-MS (*m*/*z*): 417.0 $(M - H)^-$.

Compound **7**: Yield: 89%. m.p. 200–201 °C. ^{1}H NMR (400 MHz, DMSO-d_6, 298 K) δ 10.52 (s, 2H), 7.81–7.44 (m, 12H), 4.73–4.43 (d, 8H), 2.20 (s, 6H) Elemental analysis: Calc. for $C_{28}H_{28}FeN_4O_2$: C, 66.15; H, 5.55; N, 11.02; Found: C, 66.34; H, 5.73; N, 10.96. ESI-MS (*m/z*): 507.4 $(M - H)^-$.

Compound **8**: Yield: 81%. m.p. 231–233 °C. ^{1}H NMR (400 MHz, DMSO-d_6, 298 K) δ 10.77 (s, 2H), 8.31–7.98 (m, 10H), 4.76–4.47 (d, 8H), 2.25 (s, 6H). Elemental analysis: Calc. for $C_{28}H_{26}FeN_6O_6$: C, 56.20; H, 4.38; N, 14.04; Found: C, 56.51; H, 4.09; N, 14.42. ESI-MS (*m/z*): 597.2 $(M - H)^-$.

Compound **9**: Yield: 90%. m.p. > 320 °C. ^{1}H NMR (400 MHz, DMSO-d_6, 298 K) δ 11.19 (s, 2H), 8.96–8.63 (m, 8H), 4.81–4.48 (d, 4H), 2.16 (s, 6H). Elemental analysis: Calc. for $C_{28}H_{24}FeN_8O_{10}$: C, 48.85; H, 3.51; N, 16.28; Found: C, 48.60; H, 3.72; N, 16.56. ESI-MS (*m/z*): 687.0 $(M - H)^-$.

Compound **10**: Yield: 82%. m.p. 258–261 °C. ^{1}H NMR (400 MHz, DMSO-d_6, 298 K) δ 12.10 (s, 1H), 9.67 (s, 1H), 8.76–8.73 (t, 3H), 8.17–8.01 (dd, 4H), 7.67–7.57 (m, 6H). Elemental analysis: Calc. for $C_{22}H_{16}N_2O$: C, 81.46; H, 4.97; N, 8.64; Found: C, 81.65; H, 5.09; N, 8.99. ESI-MS (*m*/*z*): 323.0 $(M - H)^-$.

Compound **11**: Yield: 79%. m.p. 307–310 °C. ^{1}H NMR (400 MHz, DMSO-d_6, 298 K) δ 12.37 (s, 1H), 9.68 (s, 1H), 8.75–8.73 (d, 3H), 8.44–8.42 (d, 2H), 8.27–8.25 (d, 2H), 8.18–8.16 (d, 2H), 7.68–7.57 (m, 3H). Elemental analysis: Calc. for $C_{22}H_{15}N_3O_3$: C, 71.54; H, 4.09; N, 11.38; Found: C, 71.29; H, 4.37; N, 11.62. ESI-MS (*m*/*z*): 368.2 $(M - H)^-$.

Compound **12**: Yield: 88%. m.p. 282–284 °C. ^{1}H NMR (400 MHz, DMSO-d_6, 298 K) δ 12.22 (s, 1H), 9.67 (s, 1H), 8.75–8.73 (d, 3H), 8.17–8.15 (d, 2H), 7.97 (s, 1H), 7.67–7.58 (t, 5H). Elemental analysis: Calc. for $C_{22}H_{14}N_4O_5$: C, 63.77; H, 3.41; N, 13.52; Found: C, 63.58; H, 3.70; N, 13.36. ESI-MS (*m*/*z*): 413.3 $(M - H)^-$.

Nanomaterials of the synthesized compounds were prepared by the reprecipitation method [37,38]. The DMSO and the water solution of CTAB (hexadecyl trimethyl ammonium bromide) were good and poor solvents, respectively. In the experiment, the good solvent containing compound (0.35 mL, 4 mmol·L^{-1}) was poured into the poor solvent containing CTAB (100 mL, 3 mmol·L^{-1}). The mixture was centrifuged for 24 h. The expected solid was washed with water and dried in a vacuum.

4. Conclusions

In conclusion, a series of new compounds (**1**–**12**) containing 1,5-diaza-fluorenone, 1,10-phenanthroline-5,6-dione, ferrocene-1,1′-dione, anthracene-9-carbaldehyde have been synthesized and the nanomaterials were also successfully developed. Probe **6** displayed the strongest binding ability for AcO^- ion among the synthesized compounds. In addition, compound **6** also illustrated wide antibacterial activity for colon bacillus, typhoid bacillus, and *Pseudomonas aeruginosa*, and inferior activity for hay bacillus and *Staphylococcus aureus*. An important clue is thus provided for the synthesis of novel compounds that have double properties, anion recognition, and antibacterial activity. Phenanthroline hydrazide derivatives can be used as potential antibacterial and anion probes.

Acknowledgments

This work was supported by the National Natural Science Foundation of China (81301269) and the Program for Science & Technology Innovation Talents administered by the Universities of Henan Province (15HASTIT039).

Author Contributions

X.F.S. designed the study and wrote the paper. W.L.L., Y.Q.F. and X.L. performed the experiments. X.F.X. performed the theoretical investigation. All authors read and approved the manuscript.

Conflicts of Interest

The authors declare no conflict of interest.

References

1. Kado, S.; Otani, H.; Nakahara, Y.; Kimura, K. Highly selective recognition of acetate and bicarbonate by thiourea-functionalised inverse opal hydrogel in aqueous solution. *Chem. Commun.* **2013**, *49*, 886–888.
2. Santos-Figueroa, L.E.; Moragues, M.E.; Climent, E.; Agostini, A.; Martínez-Máñez, R.; Sancenón, F. Chromogenic and fluorogenic chemosensors and reagents for anions. A comprehensive review of the years 2010–2011. *Chem. Soc. Rev.* **2013**, *42*, 3489–3613.
3. Shang, X.F.; Du, J.G.; Yang, W.C.; Liu, Y.; Fu, Z.Y.; Wei, X.F.; Yan, R.F.; Yao, N.C.; Guo, Y.P.; Zhang, J.L.; *et al.* The development and amino acid binding ability of nano-materials based on azo derivatives: Theory and experiment. *Mat. Sci. Eng. C* **2014**, *38*, 101–106.

4. Spence, G.T.; Chan, C.; Szemes F.; Beer, P.D. Anion binding induced conformational changes exploited for recognition, sensing and pseudorotaxane disassembly. *Dalton Trans.* **2012**, *41*, 13474–13485.
5. Schulze, B.; Schubert, U.S. Beyond click chemistry—Supramolecular interactions of 1,2,3-triazoles. *Chem. Soc. Rev.* **2014**, *43*, 2522–2571.
6. Kim, S.H; Hwang, I.J.; Gwon, S.Y.; Burkinshaw, S.M.; Son, Y.A. An anion sensor based on the displacement of 2,6-dichlorophenol-indo-*o*-cresol sodium salt from a water-soluble tetrasulfonated calix[4]arene. *Dyes Pigm.* **2011**, *88*, 84–87.
7. Yang, Z.; Zhang, K.; Gong, F.; Li, S.; Chen, J.; Ma, J.S.; Sobenina, L.N.; Mikhaleva, A.I.; Trofimov, B.A.; Yang, G. A highly selective fluorescent sensor for fluoride anion based on pyrazole derivative: Naked eye "no-yes" detection. *J. Photochem. Photobiol. A* **2011**, *217*, 29–34.
8. Lin, Q.; Cai, Y.; Li, Q.; Shi, B.B.; Yao, H.; Zhang, Y.M.; Wei, T.B. Fluorescent "turn-on" detecting CN^- by nucleophilic addition induced schiff-base hydrolysis. *Spectrochim. Acta A* **2015**, *141*, 113–118.
9. Cornes, S.P.; Davies, C.H.; Blyghton, D.; Sambrook, M.R.; Beer, P.D. Contrasting anion recognition behaviour exhibited by halogen and hydrogen bonding rotaxane hosts. *Org. Biomol. Chem.* **2015**, *13*, 2582–2587.
10. Robinson, S.W.; Mustoe C.L.; White, N.G.; Brown, A.; Thompson, A.L.; Kennepohl, P.; Beer, P.D. Evidence for halogen bond covalency in acyclic and interlocked halogen-bonding receptor anion recognition. *J. Am. Chem. Soc.* **2015**, *137*, 499–507.
11. Joo, T.Y.; Singh, N.; Lee, G.W.; Jang, D.O. Benzimidazole-based ratiometric fluorescent receptor for selective recognition of acetate. *Tetrahedron Lett.* **2007**, *48*, 8846–8850.
12. Grases, F.; March, J.G. Determination of phosphate based on inhibition of crystal growth of calcite. *Anal. Chim. Acta* **1990**, *229*, 249–254.
13. Sessler, J.L.; Cho, D.G.; Lynch, V. Diindolylquinoxalines: Effective indole-based receptors for phosphate anion. *J. Am. Chem. Soc.* **2006**, *128*, 16518–16519.
14. Furman, P.A.; Fyfe, J.A.; Clair, M.H., St.; Weinhold, K.; Rideout, J.L.; Freeman, G.A. Phosphorylation of 3′-azido-3′-deoxythymidine and selective interaction of the 5′-triphosphate with human immunodeficiency virus reverse transcriptase. *Proc. Natl. Acad. Sci. USA* **1986**, *83*, 8333–8337.
15. Velu, R.; Ramakrishnan, V.T.; Ramamurthy, P. Selective fluoride ion recognition by a thiourea based receptor linked acridinedione functionalized gold nanoparticles. *J. Photochem. Photobiol. A* **2011**, *217*, 313–320.
16. Seguí, M.J.; Lizondo-Sabater, J.; Benito, A. A new ion-selective electrode for anionic surfactants. *Talanta* **2007**, *71*, 333–338.
17. Kondo, S.; Nagamine, M.; Karasawa, S.; Ishihara, M.; Unno, M.; Yano Y. Anion recognition by 2,2′-binaphthalene derivatives bearing urea and thiourea groups at 8- and 8′-positions by UV-vis and fluorescence spectroscopies. *Tetrahedron* **2011**, *67*, 943–950.
18. Bao, X.P.; Zhou, Y.H. Synthesis and recognition properties of a class of simple colorimetric anion chemosensors containing OH and CONH groups. *Sens. Actuators B* **2010**, *147*, 434–441.
19. Sessler, J.L.; Cho, D.G.; Stepien, M.; Lynch, V.; Waluk, J.; Yoon, Z.S.; Kim, D. Inverted sapphyrin: A new family of doubly *N*-confused expanded porphyrins. *J. Am. Chem. Soc.* **2006**, *128*, 12640–12641.

20. Toraskar, M.P.; Kadam, V.J.; Kulkarni, V.M. Synthesis and antifungal activity of some azetidinones. *Int. J. Chem. Tech. Res.* **2009**, *1*, 1194–1199.
21. Khan, K.M.; Rasheed, M.; Ullah, Z.; Hayat, S.; Kaukab, F.; Choudhary, M.I.; Atta-ur-Rahman, A.; Perveen, S. Synthesis and *in vitro* leishmanicidal activity of some hydrazides and their analogues. *Bioorg. Med. Chem.* **2003**, *11*, 1381–1387.
22. Lian, S.; Su, H.; Zhao, B.; Liu, W.; Zheng, L.; Miao, J. Synthesis and discovery of pyrazole-5-carbohydrazide *N*-glycosides as inducer of autophagy in A549 lung cancer cells. *Bioorg. Med. Chem.* **2009**, *17*, 7085–7092.
23. Zhang, X.; Guo, L.; Wu, F.Y.; Jiang, Y.B. Development of fluorescent sensing of anions under excited-state intermolecular proton transfer signaling mechanism. *Org. Lett.* **2003**, *5*, 2667–2670.
24. Liu, Y.; Han, B.H.; Zhang, H.Y. Spectroscopic studies on molecular recognition of modified cyclodextrins. *Curr. Org. Chem.* **2004**, *8*, 35–46.
25. Kubo, Y.; Kato, M.; Yoshihiro Misawa, Y.; Tokita, S. A fluorescence-active 1,3-bis(isothiouronium)-derived naphthalene exhibiting versatile binding modes toward oxoanions in aqueous MeCN solution: New methodology for sensing oxoanions. *Tetrahedron Lett.* **2004**, *45*, 3769–3773.
26. Xu, Z.; Kim, S.; Lee, K.H.; Yoon, J. A highly selective fluorescent chemosensor for dihydrogen phosphate via unique excimer formation and PET mechanism. *Tetrahedron Lett.* **2007**, *48*, 3797–3800.
27. Kumar, G.S.; Neckers, D.C. Photochemistry of azobenzene-containing polymers. *Chem. Rev.* **1989**, *89*, 1915–1925.
28. Harada, J.; Fujiwara, T.; Ogawa, K. Crucial role of fluorescence in the solid-state thermochromism of salicylideneanilines. *J. Am. Chem. Soc.* **2007**, *129*, 16216–16221.
29. Liu, Y.; You, C.C.; Zhang, H.Y. *Supramolecular Chemistry*; Nankai University Publication: Tianjin, China, 2001.
30. Bourson, J.; Pouget, J.; Valeur, B. Ion-responsive fluorescent compounds. 4. Effect of cation binding on the photophysical properties of a coumarin linked to monoaza-and diaza-crown ethers. *J. Phys. Chem.* **1993**, *97*, 4552–4557.
31. Frisch, M.J.; Trucks, G.W.; Schlegel, H.B.; Scuseria, G.E.; Robb, M.A.; Cheeseman, J.R.; Montgomery, J.A., Jr.; Vreven, T.; Kudin, K.N.; Burant, J.C.; *et al*. *Gaussian03*; software for computational chemistry; Gaussian, Inc.: Pittsburgh, PA, USA, 2003.
32. Maity, D.; Bhaumik, C.; Mondal, D.; Baitalik, S. Photoinduced intramolecular energy transfer and anion sensing studies of isomeric $Ru^{II}Os^{II}$ complexes derived from an asymmetric phenanthroline-terpyridine bridge. *Dalton Trans.* **2014**, *43*, 1829–1845.
33. Ni, X.L.; Tahara, J.; Rahman, S.; Zeng, X.; Hughes, D.L.; Redshaw, C.; Yamato, T. Ditopic receptors based on lower- and upper-rim substituted hexahomotrioxacalix[3]arenes: Cation-controlled hydrogen bonding of anion. *Chem. Asian J.* **2012**, *7*, 519–527.
34. Ying, S.M.; Huang, X.H.; Luo, W.K.; Xiao, Y.C. Synthesis, crystal structures and characterizations of two homochiral coordination polymers based on a chiral reduced Schiff base ligand. *Acta Crystallogr. C Struct. Chem.* **2014**, *70*, 375–378.

35. Lee, S.A.; You, G.R.; Choi, Y.W.; Jo, H.Y.; Kim, A.R.; Noh, I.; Kim, S.J.; Kim, Y.; Kim, C. A new multifunctional Schiff base as a fluorescence sensor for Al^{3+} and a colorimetric sensor for CN in aqueous media: An application to bioimaging. *Dalton Trans.* **2014**, *43*, 6650–6659.
36. Sorna, V.; Theisen, E.R.; Stephens, B.; Warner, S.L.; Bearss, D.J.; Vankayalapati, H.; Sharma, S. High-throughput virtual screening identifies novel N′-(1-phenylethylidene)-benzohydrazides as potent, specific, and reversible LSD1 inhibitors. *J. Med. Chem.* **2013**, *56*, 9496–9508.
37. Zhang, X.J.; Zhang, X.H.; Zou, K.; Lee, C.S.; Lee, S.T. Single-crystal nanoribbons, nanotubes, and nanowires from intramolecular charge-transfer organic molecules. *J. Am. Chem. Soc.* **2007**, *129*, 3527–3533.
38. Hu, D.H.; Yu, J.; Padmanadan, G.; Ramakrishanan, S.; Barbara, P.F. Spatial confinement of excition transfer and the role of conformational order in organic nanoparticles. *Nano Lett.* **2002**, *2*, 1121–1124.